Effect of morphology on shear viscosity for binary blends of polycarbonate and polystyrene

Yuki Tanaka[1], *Takumi Sako*[1],

Tatsuhiro Hiraoka[2], *Misaki Yamaguchi*[2], *and*

Masayuki Yamaguchi[1*]

1) School of Materials Science, Japan Advanced Institute of Science and Technology,
1-1 Asahidai, Nomi, Ishikawa 923-1292, Japan

2) Hiroshima R&D Center, Mitsubishi Chemical Corporation,
20-1 Miyuki-cho, Otake, Hiroshima 739-0693, Japan

* To whom correspondence should be addressed
Phone +81-761-51-1621; Fax +81-761-51-1149
E-mail: m_yama@jaist.ac.jp

Abstract

The structure and rheological properties of binary blends of polycarbonate (PC) and polystyrene (PS) were investigated using various PS samples with different molecular weights, namely PS1k (M_w = 1000), PS53k (M_w = 53000), and PS240k (M_w = 240000). The blends with PS53k and PS240k show phase-separated structures, whereas the blend with PS1k is miscible. The shear viscosity decreases greatly on addition of PS53k and PS240k, especially at high shear rates, which would be a great advantage at processing operations. Because the non-linear response occurs in the small strain region for multilayered films of PC and PS240k, the origin of the significant viscosity drop for the phase-separated system is interfacial slippage at the phase boundary.

Keywords: Polymer blend; Rheological properties; Polycarbonate; Shear viscosity

1. Introduction

The field of polymer blends is developing in terms of both scientific understanding and industrial utility. It is well understood that a major purpose of synthesizing polymer blends is to decrease the shear viscosity to improve the processability. The addition of rubbery materials to enhance the mechanical toughness is another major target for polymer blends.[1-4] Although various blend techniques have been proposed recently to improve the processability,[5-11] there is still a strong need to reduce the shear viscosity, especially for injection molding of engineering plastics.

The miscibility between components is a key factor that determines the structure and rheological properties of polymer blends. When two polymers are thermodynamically immiscible, phase separation occurs. In the case of blends with a sea-island structure, the continuous phase greatly affects the rheological properties in the molten state, although the interfacial tension provides melt elasticity to some degree, as described by the emulsion model[12-14] and the Doi–Ohta theory.[15,16] Therefore, the addition of a low-molecular-weight compound that shows miscibility with a matrix polymer is known to be an effective method for decreasing the viscosity. In the plastic and rubber industries, therefore, plasticizers, waxes, process oils, and oligomers are usually employed to decrease the viscosity to improve the flowability.

For bisphenol-A polycarbonate (PC), which is one of the most important engineering plastics, there is a strong need to decrease the shear viscosity. Because PC has a high glass-transition temperature T_g, solidification occurs immediately in the mold in injection molding. Moreover, a recent trend to reduce product thicknesses makes it difficult to fill

65 the molten material into a mold, especially for a large product. Meanwhile, we reported
66 that the addition of polystyrene (PS) of low molecular weight decreases the shear
67 viscosity of PC. Moreover, the spiral flow length at injection molding was greatly
68 enhanced by the addition of only 5% of PS (148 mm for pure PC and 208 mm for PC/PS
69 (95/5)).[17] Although this is a novel result to the best of our knowledge, the mechanism of
70 the viscosity drop was not clarified.

71 In this study, therefore, we investigated the effect of the molecular weight of PS on
72 the rheological properties and morphology of PC/PS blends. Although conventional PC
73 and PS are known to be immiscible,[17-20] the PS sample with a low molecular weight used
74 in this study is miscible with PC. Furthermore, it should be noted that PS samples showing
75 phase separation from PC can decrease the shear viscosity greatly, especially at high shear
76 rates. The decrease is more obvious than that for the PS sample that is miscible with PC.
77 We investigated the mechanism from the viewpoint of interfacial slippage between phases.
78

79 **2. Experimental**

80 **2.1. Materials**

81 A commercially available bisphenol-A polycarbonate (PC, Iupilon S-2000,
82 Mitsubishi Chemical Engineering-Plastics, Japan) was used in this study. Three types of
83 atactic polystyrene (PS) samples of different molecular weights were employed. The
84 number- (M_n) and weight-average (M_w) molecular weights, measured by gel permeation
85 chromatography (HLC-8020, Tosoh, Japan) using chloroform as the solvent and with
86 polystyrene standard samples, are shown in Table 1. The number in the PS sample code

represents its M_w. The T_g was evaluated by differential scanning calorimetry (DSC8500, Perkin-Elmer, MA) at a heating rate of 10 °C/min.

Table 1. Characteristics of polymers

Code	M_n	M_w	M_w/M_n	T_g (°C)
PC	2.1×10^4	4.2×10^4	2.0	158
PS1k	8.7×10^2	1.0×10^3	1.2	17
PS53k	3.4×10^4	5.3×10^4	1.6	106
PS240k	9.9×10^4	2.4×10^5	2.4	112

2.2. Sample preparation

After being dried in a vacuum oven at 80 °C for 4 h, the materials were melt-mixed using an internal mixer (Labo Plastomill, 10M100, Toyo Seiki Seisakusho, Japan) at 250 °C for 6 min. The blade rotation speed was 30 rpm. The blend ratio of PC to PS was 95 to 5 by weight. The obtained blends were cut into small pieces and used for capillary extrusion measurements. Furthermore, the blends were compression-molded into flat films. After application of a pressure of 10 MPa for 4 min at 250 °C, the sample was cooled at 25 °C by a cooling unit. For reference, pure PC was subjected to the same process.

Multilayered films consisting of 20 alternating laminated films of PC and PS240k were prepared by compression-molding under the same conditions. The total thickness of the multilayered film was ca. 1 mm. Pure PC and PS films of thickness 1 mm were also prepared separately in a similar manner.

105

106 **2.3. Measurements**

107 The light transmittance of the films was evaluated by using a UV-vis
108 spectrophotometer (Lambda25, Perkin-Elmer). The refractive indices were measured by
109 using a multiwavelength Abbe refractometer (DR-M2, Atago, Japan) at 23 °C with α-
110 bromonaphthalene as the contact liquid.

111 The frequency dependences of the shear storage modulus G' and loss modulus G'' in
112 the molten state were determined using a cone-and-plate rheometer (AR2000ex, TA
113 Instruments, DE) in the angular frequency range from 0.1 to 628.3 s^{-1}. The angle of the
114 cone was 4° and the diameter was 25 mm. The linearity of the rheological response was
115 examined by measuring the strain dependence of the oscillatory shear modulus at 250 °C.
116 The shear stress σ caused by an applied strain (amplitude γ_0) at an angular frequency
117 ω was expressed by a Fourier expansion, as follows:[21,22]

118
$$\sigma = G_1'\gamma_0 \sin\omega t + G_1''\gamma_0 \cos\omega t - G_3'\gamma_0{}^3 \sin 3\omega t - G_3''\gamma_0{}^3 \cos 3\omega t + G_5'\gamma_0{}^5 \sin 5\omega t + G_5''\gamma_0{}^5 \cos 5\omega t - \cdots \quad (1)$$

119 The pressure-driven shear flow behavior was evaluated using a capillary rheometer
120 (140SAS, Yasuda Seiki Seisakusyo, Japan). Two circular dies with diameter D to length
121 L ratios (L/D) of 10/1 and 20/2 (mm/mm) were employed. The entrance angle of both
122 dies was 180°. The temperature in the barrel and die was maintained at 250 °C. The
123 measurements were performed in the shear rate range from 28 to 1000 s^{-1}.

124 The temperature dependences of the tensile storage modulus E' and loss modulus E''
125 were determined using a dynamic mechanical analyzer (Rheogel E4000, UBM, Japan) at
126 temperatures from 30 to 180 °C. The frequency and the heating rate were 10 Hz and

2 °C/min, respectively. A rectangular specimen of dimensions 20 × 5 × 0.3 mm^3 cut from the film was employed for the measurements.

Morphological observations were performed using a scanning electron microscope (SEM; S-4100, Hitachi, Japan) at an accelerating voltage of 20 kV. Both compression-molded films and extruded strands of PC/PS (95/5) were used. After cryofracturing in liquid nitrogen, the samples were immersed in cyclohexane at room temperature to dissolve the PS. Then the fractured surface was sputtered with Pt/Pd after drying. Strands were obtained from the capillary rheometer and quenched with ice water. These strands were sliced using a microtome (RX-860, Yamato Kohki, Japan) along the flow direction.

Mechanical properties in the solid state were evaluated by a uniaxial tensile machine (LSC-50/300, Tokyo Testing Machine, Japan) at 25 °C. Dumbbell-shaped specimens, cut from the compression-molded films with 300 mm thickness, were used for the measurements. One of the cross-heads of the tensile machine moved at a stretching speed of 10 mm/min. The initial gage length was 30 mm. The average value of 5 measurements was calculated for each sample.

3. Results and Discussion

The angular frequency dependences of shear storage modulus G', loss modulus G'', and complex viscosity η^* for PC, PS, and their blends are shown in Figure 1. Because of the low moduli due to their low molecular weight, G' and G'' for PS1k and G' for PS53k were not evaluated at this temperature. It was found that individual pure polymers display a typical rheological behavior in the terminal region, i.e., $G' \propto \omega^2$ and $G'' \propto \omega$.

Furthermore, the G' values of the blends with PS53k and PS240k were almost twice as high as that of pure PC at 1 rad/s, even though these PS samples show lower G' values. This behavior is explained by the emulsion model, in which the contribution of interfacial tension is considered.[12,13] In contrast, both the G' and G'' values for PC/PS1k were lower than those for pure PC across a wide range of angular frequencies, which is completely different from the other blends. The result suggests that PS1k with low viscosity is miscible with PC due to the contribution of mixing entropy and acts as a plasticizer. According to Berry and Fox, the viscosity of a polymer melt with a diluent decreases with the volume fraction of the polymer, which is provided by the following relation,[23]

$$\eta_0 = \zeta_0 \phi^{3.6} \tag{2}$$

where is ζ_0 the monomeric frictional coefficient and ϕ is the volume fraction of a polymer. A similar behavior was reported for blends of PC and poly(methyl methacrylate) of low molecular weight.[24,25]

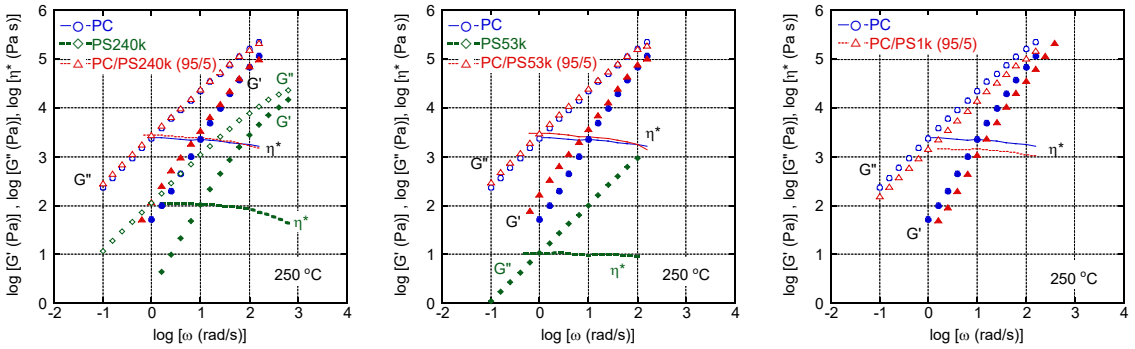

Figure 1. Frequency dependences of (closed symbols) shear storage modulus G', (open symbols) loss modulus G'', and (lines) absolute values of complex shear viscosity η^* for (circles and thin solid line) PC, (diamonds and bold dotted line) PS, and (triangles and thin dotted line) PC/PS (95/5) at 250 °C: (a) PS240k, (b) PS53k, and (c) PS1k.

168

169 These rheological properties correspond well to the blend morphologies shown in
170 Figure 2. The blends showed higher G' values in the low-frequency range (1 - 10 rad/s);
171 i.e., PC/PS240k (95/5) and PC/PS53k (95/5) clearly exhibited a phase-separated structure.
172 In contrast, phase separation was not observed in PC/PS1k (95/5) even at a high
173 magnification. Furthermore, the droplet size of PC/PS53k seems to be smaller than that
174 of PC/PS240k. The huge difference in the viscosity would be responsible for the coarse
175 morphology for PC/PS53k, as discussed by previous researchers.[26-28]

176

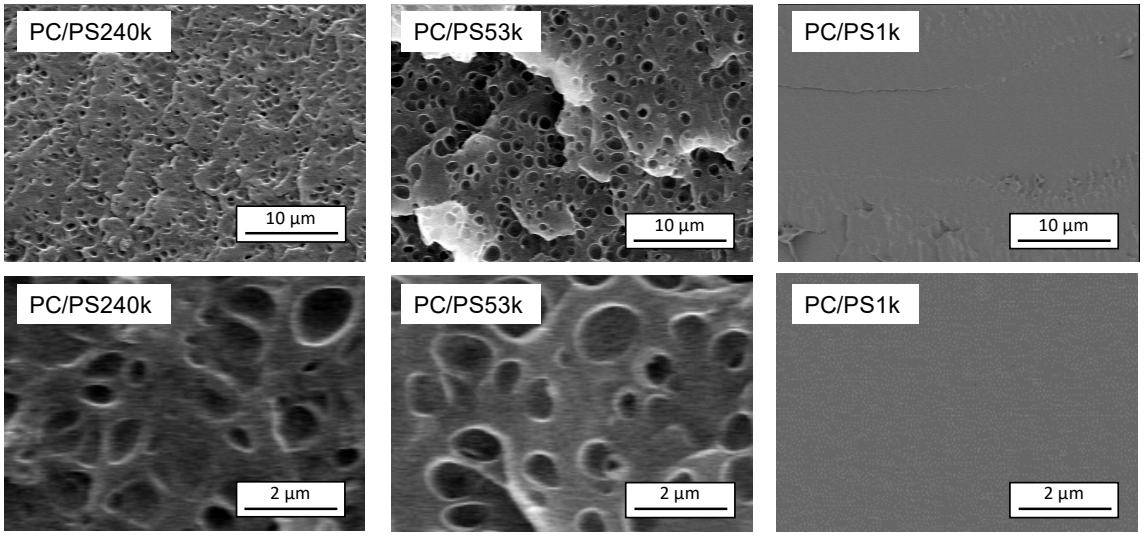

177

178 Figure 2. SEM images of PC/PS (95/5) blends: (left) PS240k, (center) PS53k, and (right)
179 PS1k.

180

181 Figure 3 shows the temperature dependences of dynamic tensile moduli such as the
182 storage modulus E' and loss modulus E'' for compression-molded films of PC and PC/PS
183 (95/5) blends. The E'' curves for the PC/PS240k and PC/PS53k blends exhibited distinct
184 double peaks, which were ascribed to the glass-to-rubber transitions of individual pure

polymers. The corresponding E' values showed step-wise decreases at 100 and 150 °C, i.e., the T_gs of PS and PC, respectively. This is reasonable because PS is known to be immiscible with PC.[17-20] In contrast, the blend with PS1k was found to be miscible, owing to the large contribution of the mixing entropy.

The molecular weight of PS necessary for it to be miscible with PC can be estimated from the Flory–Huggins interaction parameter χ. Kim and Burns calculated the χ value between PC and PS to be 0.038 ± 0.004 at 250 °C.[29] This value of the interaction parameter suggests that PS of molecular weight approximately 10000 is miscible with PC at this blend ratio (PC/PS = 95/5), which corresponds well with results in the present study (miscible with PS1k and immiscible with PS53k). Furthermore, the E' values at around room temperature for PC/PS1k were slightly higher than those for pure PC, indicating that PS1k acts as an antiplasticizer.[30,31]

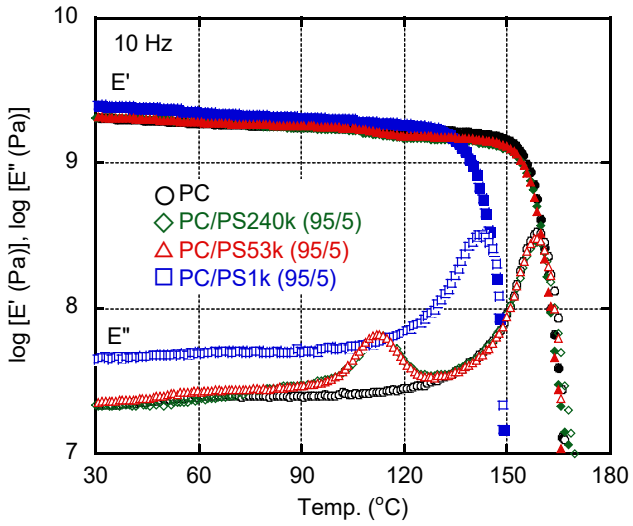

Figure 3. Temperature dependences of (closed symbols) tensile storage modulus E' and (open symbols) loss modulus E'' at 10 Hz for (circles) PC, (diamonds) PC/PS240k (95/5), (triangles) PC/PS53k (95/5), and (squares) PC/PS1k (95/5).

The light transmittances of the films are shown in Figure 4. Considering that the surface reflection R_e of both surfaces, predicted by eq. (3), was ca. 10%, the blends exhibited good transparency, irrespective of the miscibility, which is one of the reasons to employ PS as a processing modifier. Because PC and PS have almost the same reflective index across a wide range of wavelengths, as shown in Figure 5, the blend was transparent, similarly to pure PC, even when phase separation occurs as reported previously.[32,33]

$$R_e = \left(\frac{n-1}{n+1}\right)^2 \tag{3}$$

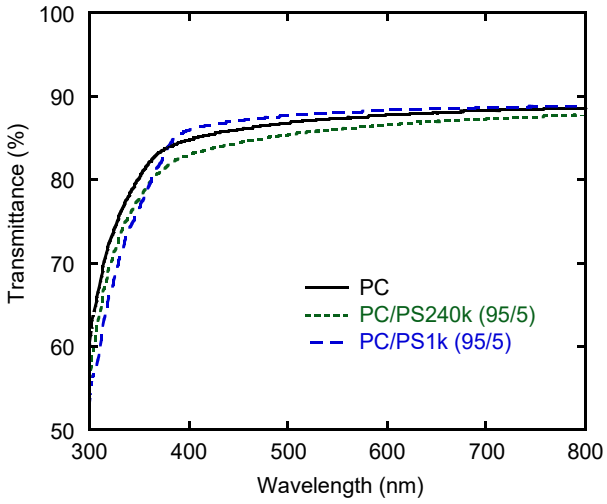

Figure 4. Light transmittances in the visible wavelength for PC, PC/PS240k (95/5), and PC/PS1k (95/5) films of thickness 300 μm.

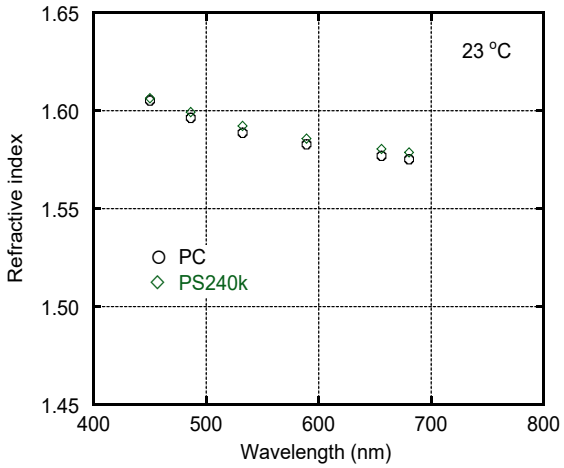

Figure 5. Refractive indices of PC and PS240k.

Although the linear viscoelastic properties suggested that PS240k and PS53k do not have any plasticization effect on the linear viscoelasticity of PC, we observed a significant viscosity decrease by performing capillary extrusion measurements. The flow curves for PC, PS240k, PC/PS240k (95/5), PC/PS53k (95/5), and PC/PS1k (95/5), which were constructed with data obtained by using a capillary rheometer with a circular die (L = 10 mm, D = 1 mm) at 250 °C, are shown in Figure 6, in which the apparent values on the wall are plotted for both the shear rate $\dot{\gamma}$ and steady-state shear viscosity η.

The shear viscosity of PC/PS1k (95/5) at a low shear rate was lower than those of the other blends. This is a typical flow curve for plasticized polymer systems.[34,35] In contrast, pronounced viscosity drops were observed at a high shear rate on addition of PS240k and PS53k, and the drops were much more prominent than that caused by PS1k. In general, the shear viscosity of an immiscible blend is dominated by that of the continuous phase. Therefore, a great decrease in the shear viscosity is not expected on addition of an immiscible polymer. Therefore, the experimental result is noteworthy. Of

course, the Cox-Merz empirical rule is not applicable for the immiscible blend systems.

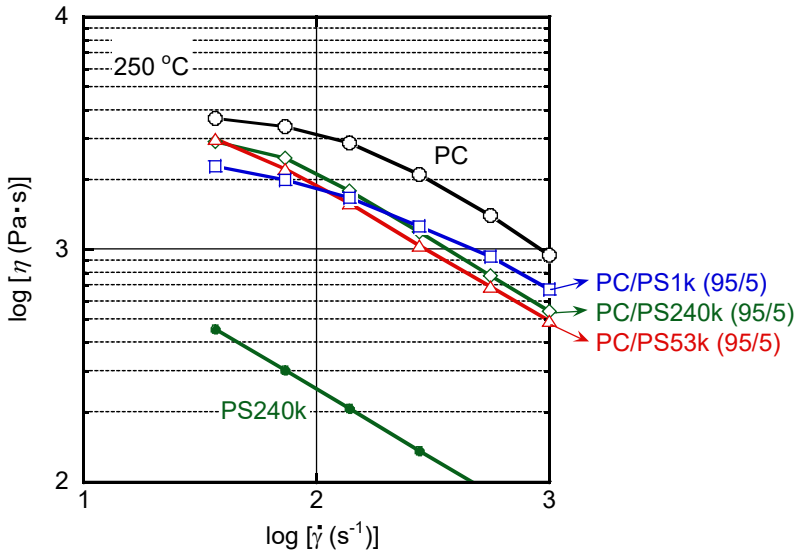

Figure 6. Shear rate dependences of shear viscosities for PC, PS240k, PC/PS240k (95/5), PC/PS53k (95/5), and PC/PS1k (95/5).

In capillary extrusion measurements, wall slippage can be the origin of an apparent viscosity decrease. The slippage can be evaluated by Mooney's method, by using various dies with different diameters and the same L/D ratios.[36,37] Figure 7 shows the flow curves obtained using two dies with the same L/D ratio (10/1 and 20/2). When slippage takes place, the apparent shear stress measured by the die with the smaller diameter is lower than that obtained by the die with the larger diameter. However, in the case of our measurements, the flow curves obtained by the different dies are identical, demonstrating that the viscosity decrease is not attributable to slippage on the wall. Furthermore, the extruded strands have a smooth surface without any distortion; i.e., flow instabilities, such as shark-skin failure and gross melt fracture, do not take place.

249

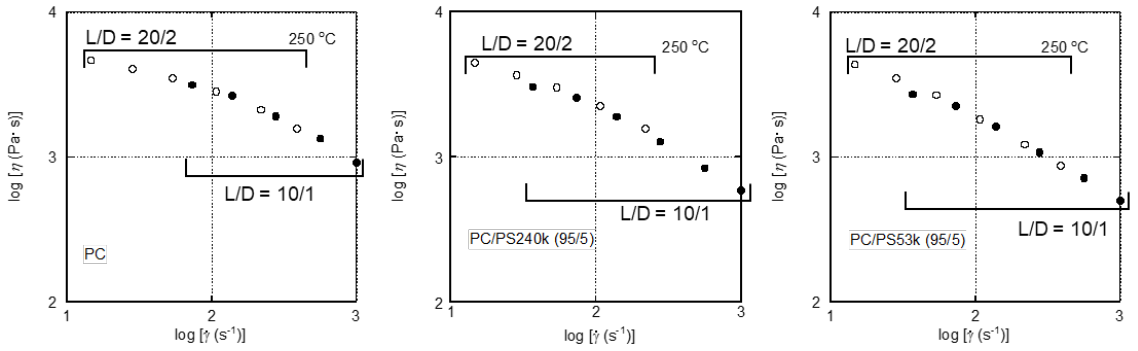

250

251 Figure 7. Apparent shear viscosity η on wall at 250 °C for (left) PC, (middle) PC/PS240k,
252 and (right) PC/PS53k, obtained by two capillary dies with the same L/D ratio: (closed
253 symbols) L/D = 10/1 and (open symbol) L/D = 20/2.

254

255 Figure 8 shows SEM images of the core region in cross-sections of PC/PS strands
256 along the flow direction, extruded from a circular die with an L/D ratio of 10/1 at 250 °C.
257 The apparent shear rates on the wall were 73 s^{-1} and 1000 s^{-1}. At both shear rates, no
258 phase-separated structure was detected in strands of PC/PS1k. In contrast, spherical
259 droplets of PS were observed for PC/PS240k and PC/PS53k at 73 s^{-1}. Furthermore,
260 deformed small particles aligned with the flow direction, which must be generated by the
261 disintegration of deformed droplets arising from the Rayleigh disturbance,[38,39] appear at
262 1000 s^{-1}. Since the Rayleigh disturbance occurs after the cessation of flow, PS droplets
263 are greatly deformed in the flow direction, leading to a pronounced interfacial area.

264

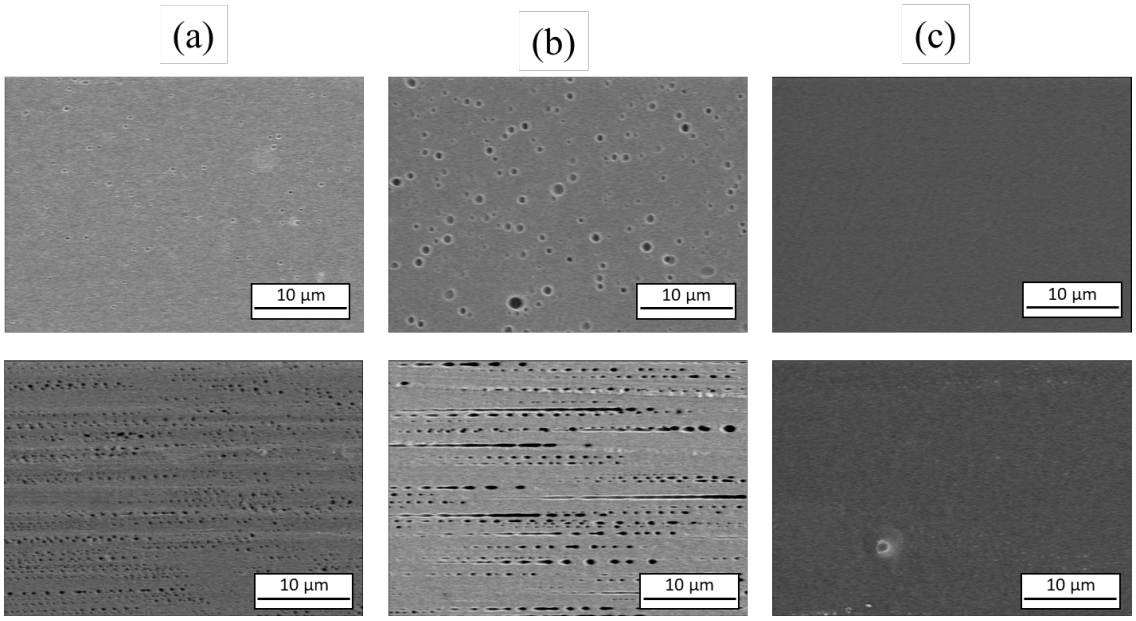

Figure 8. SEM images of extruded strands for blends of (a) PC/PS240k (95/5), (b) PC/PS53k (95/5), and (c) PC/PS1k (95/5) at (top) 73 s^{-1} and (bottom) 1000 s^{-1}.

The strain dependence of the oscillatory shear modulus was evaluated to clarify the mechanism of the huge viscosity drop for the immiscible blends. The oscillatory moduli in the non-linear region were obtained by using a Fourier expansion. The samples were prepared by laminating 20 films, even for pure PC. In the case of the laminated sample PC–PS240k, 20 films of both PC and PS240k were alternately piled and compressed at 250 °C. Figure 9 shows the strain dependences of G_1' and G_1'' normalized by the G' and G'' values, respectively, in the linear viscoelastic region.

It was apparent that the maximum strain needed to show linearity is smaller for the layered sample, i.e., PC–PS240k, than those for PC and PS at any frequency. The origin of the non-linearity for the layered sample is interfacial slippage. This is reasonable because the interfacial thickness between immiscible polymers is significantly thin, leading to interfacial slippage, as demonstrated by multilayered extrusion.[40-42] Such

slippage should occur even in blend systems during capillary extrusion and must be pronounced at high shear rates because of the high shear stress. The results suggested that the significant viscosity drop in the high shear rates of the phase-separation system is attributable to polymer–polymer interfacial slippage.

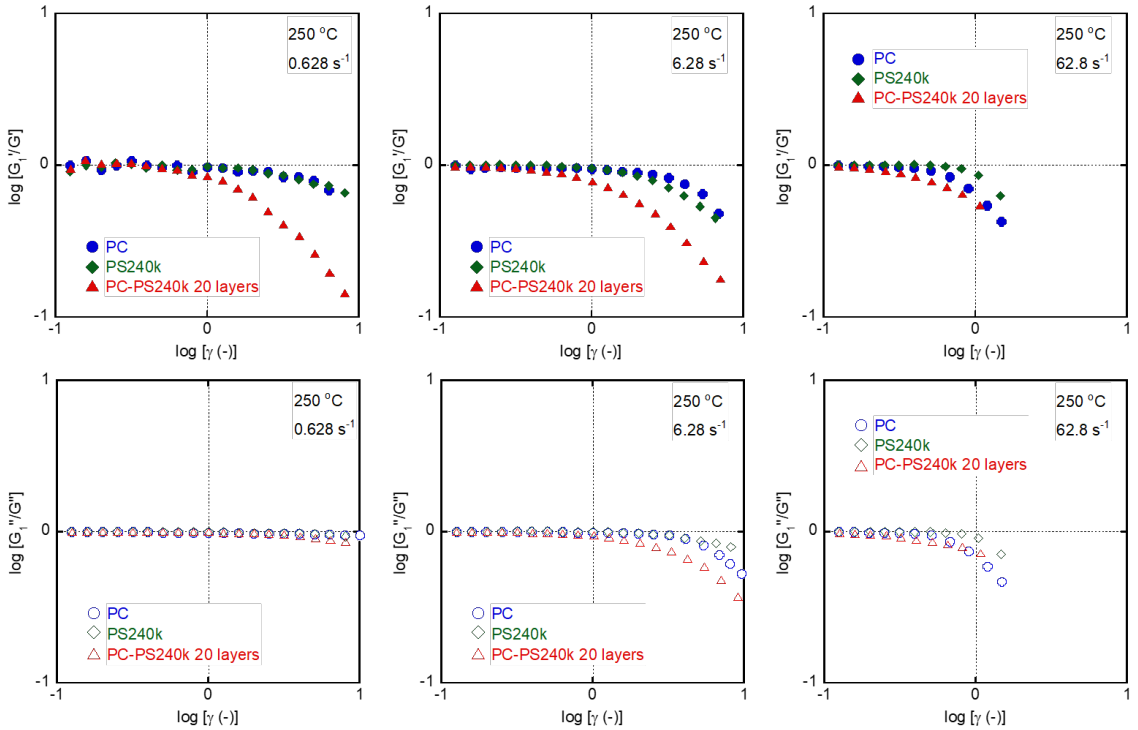

Figure 9. Strain dependences of (top) G_1'/G' and (bottom) G_1''/G'' for PC, PS240k, and their multilayered film, i.e., PC–PS240k, at (left) 0.628, (center) 6.28, and (right) 62.8 s^{-1}.

The adhesive strength between phases must be determined by the interfacial thickness λ, which has a close relationship with the interaction parameter χ as follows,[43-45]

$$\lambda = \frac{2l_K}{(6\chi)^{1/2}} \quad (4)$$

where l_K is the segment length.

Since the segment length of PS is 1.67 nm (ref.46) and the interaction parameter between PC and PS is 0.038 at 250 °C,[29] the interfacial thickness is calculated to be 7.0 nm. Considering that the entanglement spacing, i.e., tube diameter, of PS is around 8.5 nm,[47] the interfacial thickness is too thin to show the adhesive strength. Although it is still unknown that such phenomenon can be detected for other blend systems, the weak boundary and greatly deformed dispersions with large interface would play an important role on this viscosity drop.

Considering the industrial application, the stress-strain curves in the solid state were evaluated as shown in Figure 10. Both stress and strain in the figure are the engineering values. Furthermore, the average values of yield stress and strain at break are summarized in Figure 11.

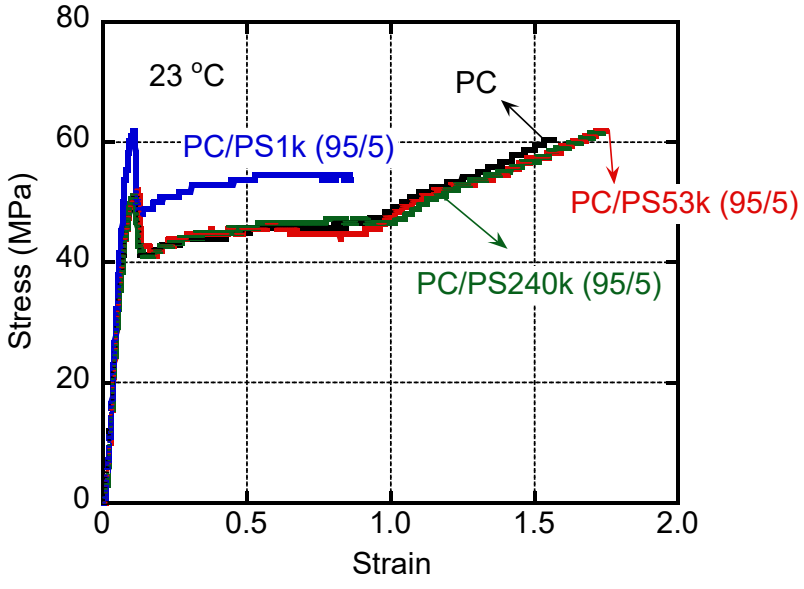

Figure 10. Stress-strain curves for PC, PC/PS240k (95/5), PC/PS53k (95/5), and PC/PS1k (95/5).

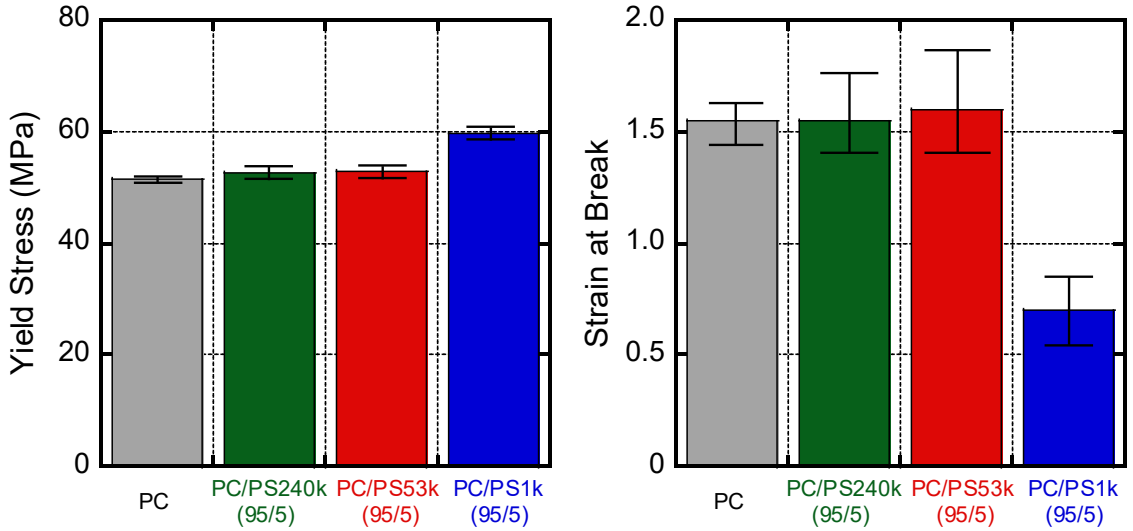

Figure 11. Yield stress and strain at break for PC, PC/PS240k (95/5), PC/PS53k (95/5), and PC/PS1k (95/5).

Although PC is known to exhibit a good mechanical toughness, the addition of PS1k decreased the strain at break. This is attributed to the antiplasticized effect.[30,31] In fact, the modulus (see Figure 3) and yield stress were obviously enhanced by the PS1k addition. In contrast, the addition of PS53k and PS240k barely affect the tensile properties greatly at this blend ratio. In future, we should evaluate the impact strength for industrial applications, because it is one of the most attractive properties for PC.

4. Conclusions

The effect of PS addition on the rheological properties of PC was studied using PS samples with various molecular weights. It was found from the dynamic mechanical properties and SEM observations that PS1k is miscible with PC, whereas PS53k and

PS240k are immiscible. It should be noted that addition of PS53k and PS240k resulted in a marked viscosity drop, especially at high shear rates. Moreover, the mechanical properties are hardly affected. Therefore, the rheology modification only by 5% of PS must be recognized as a novel method, which could be applicable for actual processing operations.

It was found from the strain dependences of the oscillatory shear moduli that a multilayered film composed of PC and PS240k shows non-linearity in the small strain region, unlike pure PC and PS240k. The non-linear response detected for the multilayered film must be attributed to interfacial slippage between PC and PS. This interfacial slippage should occur in the immiscible blends under capillary flow, and is responsible for the anomalous viscosity drop at high shear rates.

Acknowledgements

A part of this work was supported by JSPS Grant-in-Aid for Scientific Research (B) Grant Number 16H04201.

References

1. Utracki, L. A. Polymer alloys and blends; Thermodynamics and rheology, Hanser: Munich, **1990**.
2. Robertson, L. M. Polymer blends; A comprehensive review, Hanser: Munich, **2007**.
3. Münstedt, H. Rheological and morphological properties of dispersed polymeric materials, Hanser: Munich, **2016**.

4. Yamaguchi, M. Manufacturing of high performance biomass-based polyesters by rheological approach. In Handbook of composite from renewable materials, Thakur, V. K.; Thakur, M. K. Eds., Chap. 2, John Wiley & Sons: New York, **2016**.
5. Yamaguchi, M.; Miyata, H. *Polym. J*. **2006**, *32*, 164-170.
6. Yamaguchi, M.; Wakabayashi, T. *Adv. Polym. Technol*. **2006**, *25*, 236-241.
7. Yokohara, T.; Nobukawa, S.; Yamaguchi, M. *J. Rheol*. **2011**, *55*, 1205-1218.
8. Yamaguchi, M.; Yokohara, T.; Ali, M. A. B. *Nihon Reoroji Gakkaishi*, **2013**, *41*, 129-135.
9. Seemork, J.; Sako, T.; Ali, M. A. B.; Yamaguchi, M. *J. Rheol*. **2017**, *61*, 1-11.
10. Fujii, Y.; Nishikawa, R.; Phulkerd, P.; Yamaguchi, M. *J. Rheol*. **2019**, *63*, 11-18.
11. Otsuki, Y.; Fujii, Y.; Sasaki, H.; Phulkerd, P.; Yamaguchi, M. *Polym. J*. **2020**, *52*, 529-538.
12. Graebling, D.; Muller, R.; Palierne, J. F. *Macromolecules*, **1993**, *26*, 320-329.
13. Palierne, J. F. *Rheol. Acta* **1990**, *29*, 204-214.
14. Yamaguchi, M.; Miyata, H. *Macromolecules* **1999**, *32*, 5911-5916.
15. Doi, M.; Ohta, T. *J. Chem. Phys*. **1991**, *95*, 1242-1248.
16. Takahashi, Y.; Kitade, S.; Kurashima, N.; Noda, I. *Polym. J*. **1994**, *26*, 1206-1212.
17. Sako, T.; Date, J.; Hagi, H.; Hiraoka, T.; Matsuoka, S.; Yamaguchi, M. *Polymer* **2019**, *170*, 135-141.
18. Cheng, J.; Chen, Z.; Zhou, J.; Cao, Z.; Wu, D.; Liu, C.; Pu, H. *Appl. Surface Sci*. **2018**, *44*, 946-954.
19. Wisniewski, C.; Marin, G.; Monge, Ph. *Eur. Polym. J.* **1985**, *21*, 479-484.

371 20. Chuai, C. Z.; Almdal, K.; Johannsen, I.; Lyngaae-Jørgense, J. *Polym. Eng. Sci.* **2002**,
372 *42*, 961-968.
373 21. Onogi, S.; Masuda, T.; Matsumoto, T. *Trans. Soc. Rheol.* **1970**, *14*, 275-294.
374 22. Matsumoto, T.; Segawa, Y.; Masuda, T.; Onogi, S. *Trans. Soc. Rheol.* **1973**, *17*, 47-
375 62.
376 23. Berry, G. C.; Fox, T. G. *Adv. Polym. Sci.* **1968**, *5*, 261-357.
377 24. Sako, T.; Nobukawa, S.; Yamaguchi, M. *Polym. J*. **2015**, *47*, 576-579.
378 25. Sako, T.; Ito, A.; Yamaguchi, M. *J. Polym. Res*. **2017**, *24*, 89-93.
379 26. Kargar-Kocsis, J.; Kallo, A.; Kuleznev, V. N. *Polymer*, **1984**, *25*, 279-287.
380 27. Favis, B. D.; Chalifox, J. P. *Polym. Eng. Sci.*, **1987**, *27*, 1591-1600.
381 28. Wu, S. *Polym. Eng. Sci.*, **1987**, *27*, 335-343.
382 29. Kim, W. N.; Burns, C. M. *J. Appl. Polym. Sci.* **1987**, *34*, 945-967.
383 30. Nielsen, L. E.; Landel, R. F. Mechanical properties of polymers and composites, 2nd
384 ed., CRC Press; New York, **1994**.
385 31. Miyagawa, A.; Korkiatithaweechai, S.; Nobukawa, S.; Yamaguchi, M. *Ind. Eng.*
386 *Chem. Res.* **2013**, *52*, 5048-5053.
387 32. Takahashi, S.; Okada, H.; Nobukawa, S.; Yamaguchi, M. *Eur. Polym. J.*, **2012**, *48*,
388 974-980.
389 33. Kuhakongkiat, K.; Sugiyama, M.; Guesnier, M.; Azaman, F. A.; Yoshida, K.;
390 Yamaguchi, M. *J. Appl. Polym. Sci.*, **2017**, *135*, 45927.
391 34. Berry, G. C.; Fox, T. G. *Adv. Polym. Sci*. **1968**, *5*, 261-357.
392 35. Huang, T.; Miura, M.; Nobukawa, S.; Yamaguchi, M. *J. Polym. Environ*. **2014**, *22*,

183-189.

36. Mooney, M. *J. Rheol*. **1931**, *2*, 210-222.

37. Larson, R. G. The structure and rheology of complex fluids, Oxford University Press; New York, **1988**.

38. Macosko, C. W. Rheology: Principles, measurements, and applications, Wiley; New York, **1994**.

39. Oosterlinck, F.; Vinckier, I.; Mours, M.; Laun, H. M.; Moldenaers, P. *Rheol. Acta* **2005**, *44*, 631-643.

40. Brochard, F.; de Gennes, P. G. *Langmuir*, **1992**, *8*, 3033-3037.

41. Zhao, R.; Macosko, C. W. *J. Rheol*. **2002**, *46*, 145-167.

42. Lee, P. C.; Park, H. E.; Morse, D. C.; Macosko, C. W. *J. Rheol*. **2009**, *53*, 893-915.

43. Helfand, E.; Tagami, Y. *J. Polym. Sci., B, Polym. Phys. Ed.*, **1971**, *9*, 741-746.

44. Helfand, E.; Tagami, Y. *J. Chem. Phys*., **1971**, *56*, 3592-3599.

45. Yamaguchi, M. *J. Appl. Polym. Sci.*, **1998**, *70*, 457-463.

46. Van Krevelen, D. W.; te Nijehuis, K. Properties of polymers 4th ed.; Elsevier: Amsterdam, **2009**.

47. Fetters, L. J.; Lohse, D. J.; Colby, R. H. Chain dimensions and entanglement spacings; In Physical properties of polymers handbook, 2nd ed., Ed.; Mark, J. E.; Springer: New York, **2007**; Chap.23.